A Novel Visualization Method of Vessel Network for Tumour Targeting: A Vessel Matrix Approach

Mengsheng Zhai[1], Minghao Liu[2], Zhijing Wang[3], Yifan Chen[2,4(✉)], and Yue Sun[2,5(✉)]

[1] School of Optoelectronic Science and Engineering, University of Electronic Science and Technology of China, Chengdu, China
[2] School of Life Science and Technology, University of Electronic Science and Technology of China, Chengdu, China
[3] Glasgow College, University of Electronic Science and Technology of China, Chengdu, China
[4] Yangtze Delta Region Institute (Huzhou), University of Electronic Science and Technology of China, Chengdu, China
yifan.chen@uestc.edu.cn
[5] School of Mechanical and Electrical Engineering, Chengdu University of Technology, Chengdu, China
sunyuestc90@126.com

Abstract. When the tumour grows, the microvessel density in the surrounding area increases and exhibits irregular curvature, which shows a difference from the regular vascular network. Therefore, a model is needed to describe the vascular network around the tumour. However, the existing models can not provide a good representation of the vascular network. This paper proposes a Vessel Matrix Model (VMM), a visualization vascular network model which has the potential to resemble the complicated vessels networks around the tumour microenvironment. VMM is conducive to the works such as drug delivery and tumour search and can perform a tumour-targeting search by combining with the computational nanobiosensing (CONA) framework. CONA uses nanorobots as computing agents to learn the surrounding environment to regulate the path-planning to the tumour location through algorithms such as reinforcement learning. A CONA method is performed in searching for a tumour to verify the feasibility of this vascular network. In order to seek optimal routing in the vascular network, VMM provides distance reward and weight reward for the agents, where the rewards are determined by the distance of starting point to the tumour lesion and the gradient of BGF, respectively. Therefore, VMM enables the tumour search with the CONA method. By introducing different weights between the destination and weights rewards, it is found that targeting efficiency can be affected by branch rate and size of the network.

M. Zhai and M. Liu—These authors contributed to the work equally and should be regarded as co-first authors.

Y. Chen et al. (Eds.): BICT 2023, LNICST 512, pp. 40–49, 2023.
https://doi.org/10.1007/978-3-031-43135-7_5

Keywords: tumour targeting · Vessel Network Visualization · Reinforcement learning · Vessel Matrix Model · CONA

1 Introduction

Cancer is regarded as abnormal and uncountable cell growth due to the specific genetic accumulation, which is the primary factor that results in fatal death globally [1,2]. As a result, clinical diagnosis is needed to detect cancer at an early stage [3]. Nevertheless, traditional medical imaging technology, such as MRI and CT, has a significant challenge since the resolution and information acquired by these facilities are restricted.

With the advances in nanotechnology, nanomedicines, using nanoparticles, are considered a new solution to prevent and treat disease. For decades, researchers have been working on developing nanoparticles that can accurately detect tumours and deliver drugs to cancer lesions. However, just 0.7 percent of the nanoparticles' injected dose (ID) can be delivered to tumour targets without external guidance, and delivery efficiency has not increased significantly in the last decade [4]. Therefore, recent years have made immense progress on the externally controllable nanobots, which can be manipulated by an external magnetic field, in the *in vivo* environment [5]. Utilizing the manipulable nanorobots in tumour targeting and drug delivery, as a result, we propose a novel computational nanobiosensing (CONA) framework. In addition, the performance of autonomous nanorobots achieved considerable high targeting efficiency [6]. These types of nanorobots have ability to explore the *in vivo* environment using reinforcement learning [7]. Besides, the biological gradient field (BGF) is introduced to this model, and through the principles of cooperation and coordination, the sensing nanoparticles successfully find the target. Internal structural changes generated by *in vivo* physical, chemical, or biological perturbations in the peritumoral area allow these nanoparticles to perform target-directed motility [8].

In our previous work [10,11], the drug delivery process is mapped into Molecular Communication (MC). The vessel network is regarded as the communication channel from NPs released site to the tumour lesions. The impulse response of the blood vessel-based communication channel contributes to the calculation of the drug concentration at the received end, which indicates a quantified drug delivery system. Therefore, a visualization vessel model is needed for drug delivery and tumour targeting applications. Recently, there have been proved that natural blood vessels can be transformed into the form of matrices utilizing images, which lays the foundation for a more realistic simulation of blood vessels. Based on this, this paper proposes Vascular Matrix Model (VMM), a method for describing blood vessels using a matrix combined with CONA to guide agents to target tumours. VMM may continue to display more features of the vascular network in the future, such as the transition model from fractal to lattice.

This paper is organized as follows. Section 2 describes the vascular matrix model. In Sect. 3, methodology including the Markov decision process, the allocation of values is introduced. Following that, simulations based on this model

are presented, and the results are shown in Sect. 4. Finally, Sect. 5 shows the major outcomes and the conclusion is drawn.

2 The Vessel Matrix Model

The VMM assumes blood vessels are equivalent to matrices. The idea is inspired from [12], where they have proved that it is feasible for the robot to accomplish route path-planning using a matrix.

Given the complexity of blood vessels in the human body, only one matrix can not well generalize the topography of blood vessels. We use the following matrices to simulate the blood vessels:

- H_{label} represents the state of blood vessel i and j. For each element,

$$x_{ij} = \begin{cases} 1, & \text{two blood vessels are connected} \\ 0, & \text{two blood vessels are blocked} \end{cases} \tag{1}$$

- H_{loc} represents the distance from blood vessels i and j. In the matrix, the elements indicate where the vessel is connected.
- H_{weight} represents the information of BGF for the branch of each blood vessel. Some vessels may have a high value of BGF, so their weight must be greater than others and more valuable for the agent.

It has been proved that it is achievable to extract real blood vessels into the form of matrices based on vessel images [13], which is shown in Fig. 1, revealing the mapping from the vessel to the matrix.

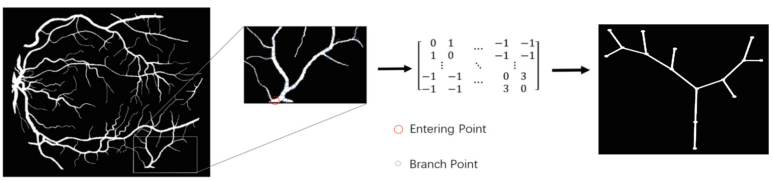

Fig. 1. Generating matrices from blood vessels images. The H_{label} matrix can be generated by transforming the blood vessels images to define the connectivity of the blood vessels.

We use the VMM model to reconstruct the blood vessel model corresponding to the medical image, in which two matrices H_{loc} and H_{weight} are used to describe the weights and the length of vessel branches. The result is shown in Fig. 2.

However, it lacks vessel datasets to train the model, so the following guidelines are used to generate the training datasets:

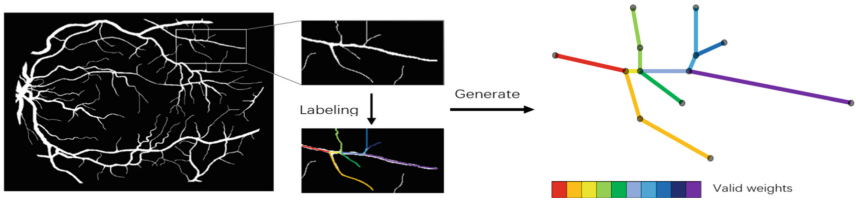

Fig. 2. Schematic diagram of the blood vessel model generated by the VMM model. Different weights of BGFs information are represented by different colors.

1. Select a size for the matrix H_{label} and initialize the matrix.
2. Initialize branch rate r which refers to the degree of branching of blood vessels.
3. Generate a random integer $r_{x_{ij}}$ and compare the $r_{x_{ij}}$ with the branch rate r. If $r_{x_{ij}}$ is greater than r, set the value to 1; otherwise, set it to 0.
4. Repeat step 3) until all points has been iterated and computed.
5. Initialize the matrix H_{loc} which has the same size of H_{label} and generate a random integer for each element x_{ij} in H_{loc} whose value in H_{label} is 1.
6. Initialize the matrix H_{weight} which has the same size of H_{label} and generate a random integer for each element x_{ij} in H_{weight} whose value in H_{label} is 1.

3 Tumour Searching Method

In the simulation process, the nanorobots detected the position of tumours in a grid-like vascular network of a given size. The core goal is to locate the tumor with a minimum exploring path. This problem is considered an optimization of the reward function, which uses the Markov decision process (MDP).

3.1 Markov Decision Process

The aforementioned problem is formulated as an MDP [14]. In this process, the definition (S, A, R) is represented separately as state space, action space, and reward function. The state at mission time t in the vascular network is given by $s_t = (p_t, p_t) \in \mathbb{R}^2$, which is the position of the nanorobots. Nanorobots are allowed to take the following actions:

$$A_{ij} = \{1, 2, 3, ..., n\} \tag{2}$$

where n is the number of branches from x_{ij}.

If the nanorobots collide with a vessel wall, they enter idle mode; otherwise, they move ahead in one of the four directions defined in the equation (2). The state-actions are mapped to a real-valued reward using the reward function, i.e., S $\times$ A $\rightarrow$ R.

3.2 Value Allocating

It is necessary for the agent to have reward, action, value, and states in order to train and update the Reinforcement Learning (RL) algorithm. So, it is critical to allocate the value for the agent, the rule of allocated value will be proposed.

Value of Destination. In order to describe the value of the destination for our agent, we use the Dijkstra algorithm to find the shortest distance from the destination. The calculated shortest path is stored in the $Dis(x_i)$ array, where x_i is the index of the distance array.

According to the Dijkstra algorithm [13], we follow these steps to find the shortest distances:

1. Initialize the matrix and select a point x_i from the matrix. The array Dis initializes with the distance the x_i contained.
2. The array r_{ix}, and select a point x_i from the matrix. The array Dis now contains some distances, and we select the shortest one x_j to continue our search.
3. Comparing the array Dis with the current distance from the point x_j which the distance has added the $Dis(x_j)$, and keeping the miniature data into the array Dis.
4. Repeat step 2) until all points have been iterated and computed

When the shortest distance is available, we have the following steps to compute the value of the destination.

$$V_{dst} = [Dis(X_n) - Dis(X_c)]V_0 \tag{3}$$

where $Dis(X_n)$ and $Dis(X_c)$ represent the distance from the current location and the next location to the destination, respectively. The last parameter V_o is the offset value for the V_{dst}.

Value of Weights in Vessel. By introducing H_{weight} and H_{loc}, the value of weights could be described in following equation.

$$V_{weight} = \begin{bmatrix} z_{1,1} & z_{1,2} & \cdots & z_{1,j} \\ z_{2,1} & z_{2,2} & \cdots & z_{2,j} \\ \vdots & \vdots & \ddots & \vdots \\ z_{i,1} & \cdots & \cdots & z_{i,j} \end{bmatrix}, \tag{4}$$

$$z_{i,j} = \frac{x_{i,j}}{y_{i,j}} \tag{5}$$

where $x_{i,j}$ and $y_{i,j}$ are elements at corresponding positions in matrix H_{weight} and matrix H_{loc}, respectively.

V_{weight} could be equivalent to the gradient of BGF. The greater V_{weight} is, the more valuable for the agent this area is.

Value in Total. Let V_{total} denote the value in total, which contain both V_{dst} and V_{weight}. In case of an imbalance value's negative impact on the agent, some biases are used to balance the values. Here we write the equation as the following equation:

$$V_{total} = aV_{dst} + bV_{weight}, \tag{6}$$

where the parameter a and b are the rates to weight the value for the parameter V_{dst} and V_{weight}.

3.3 Deep Q-Network

Due to the complexity of the vascular network, the number of states of the agent may be very large. Therefore, Q-learning in RL will result in the exponential growth of the Q-table, we adopt DQN to train agents to learn in CONA.

The DQN (Deep Q-Network) algorithm is a neural network architecture for model-free reinforcement learning [15]. It successfully realizes the end-to-end from perception to action and has been applied in gaming and navigation. The DQN algorithm introduces deep learning into reinforcement learning, in which the interaction between the nanorobots agent and the environment enables the agent to learn and optimize its behaviour. The learning process is evaluated by improving the Q-function iteratively. The computation and updating of the Q-function can be written as the following equation:

$$Q(s,a) \leftarrow Q(s,a) + \alpha[r + \gamma \max_{a'} Q(s',a') - Q(s,a)] \tag{7}$$

where s is the agent state which includes the overall situation of the whole vessel, a is the action performed by the agent, and r represents the reward to the agent. The constants α and γ are the learning rate and decaying rate, which control the convergence rate of the agent and the impact factor from the future. Practically, DQN's neural network (NN) weights should be updated by the gradient of its loss function:

$$L(\theta) = E[T_Q - Q(s,a;\theta)^2] \tag{8}$$

where T_Q is the optimization objective, which is calculated as follows:

$$T_Q = r + \gamma \max_{a'} Q(s',a';\theta) \tag{9}$$

3.4 Target Network

The target network is used to generate a T_Q for the main NN so that the main NN could update its NN weights according to the gradient for a period of iterations, and we set it 100 times here. The loss is counted by the quality of the main NNQ and the T_Q. Such a measure can reduce the relevance between Q and T_Q, usable for increasing the stability of DQN.

3.5 Experience Replay

DQN proposes a buffer in which the agent would randomly select the situation to train itself. In our work, the environment information and the action generated by the agent are stored in a buffer. While training, the agent selects a batch of buffers to review the past situation to train itself. As a result, the lack of relevance with samples and its problem of non-static distribution is partially compensated. Hence, experience replay can improve the robustness of the NN.

4 Simulation and Results

4.1 Simulation Setup

According to the input state, DQN model calculates the reward of each vessel branch. As a result, the vessel branch with the highest reward will be selected. The action is invalid when the action calculated according to the reward is marked as impassable in the H_{label}. To correct this action, we propose two methods.

1. Return a false result when the output is invalid so that the agent can learn and act accordingly. However, massive training is needed in this method and hardly ensures efficiency.
2. Execute a random action when the action is invalid. Although this method cannot guarantee accuracy, it does not need massive training.

Therefore, the second method is utilized to test the proposed VMM model. In the simulation, we set the total test time to 50'000 times to eliminate the effect of random movement in different circumstances. Considering the limited lifespan of the nanorobot, we set the maximum detection time as 100. Sessions that do not reach the end within the time will be considered invalid.

We changed the vascular branch rate and the number of vascular branches in the VMM model to simulate different vascular environments, as shown in Fig. 2. Set the parameters in the simulation as follows: $\gamma = 0.9$, $V_0 = 60$.

4.2 Different Scenarios

The result of the different branches generating probabilities r and different sizes is compared in a single circumstance. As shown in Fig. 3, each circumstance has a good efficiency in finding the tumour. From the found times and found rate data, we notice that the agent's efficiency mainly depends on the number of branches and size of the vascular network.

According to equation (7), we know that the process of searching for tumours is affected by both reward V_{dst} and V_{weight}, so the parameter $\beta = \mathrm{a/b}$ is set to play a role in regulating the relative weight of the two rewards in the simulation. As the weight, β increases from 0.01 to 100, the number of found times and found rate do not show significant differences, which indicates that searching efficiency is less affected by β.

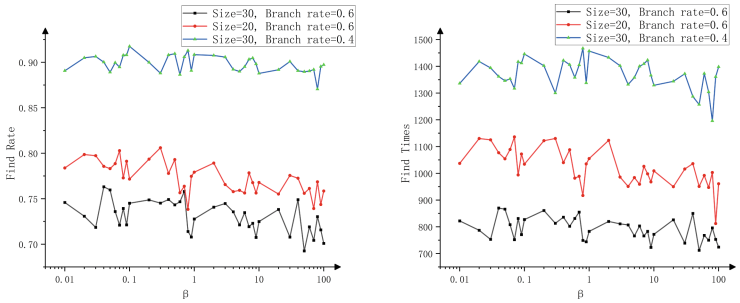

Fig. 3. Found times (a) and found rates (b) for different branch generate probabilities r and different sizes when model converged, the log of β is taken.

The fluctuation of reward can reflect the stability of the search process, and a huge reward indicates that the search process is greatly affected by random actions. As shown in Fig. 4, when the value of beta is too high, the standard deviation of the reward increases significantly, and the learning effect of the neural network is not good. When the value of β is too low, it is not in line with the actual situation in the human body, so the value of β should be considered by considering the above factors and making a compromise.

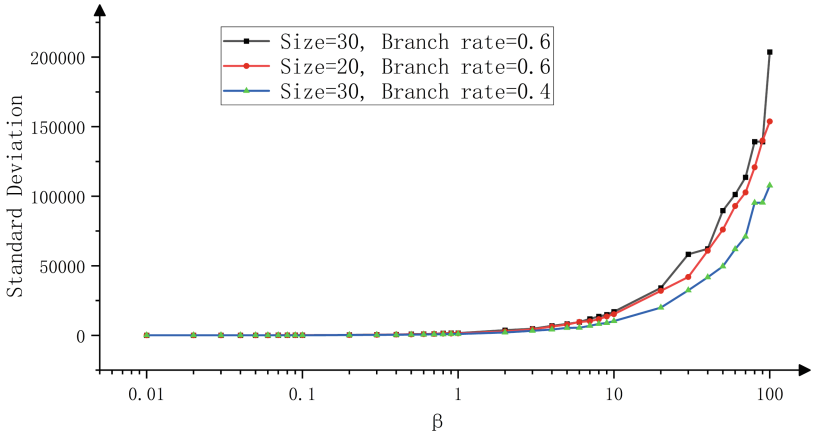

Fig. 4. The standard deviation of total reward when model converged, the log of β is taken.

5 Conclusion

We proposed a novel model for displaying blood vessels that can be used to expand tumour sensitization and tumour targeting. The major contributions are as follows:

- This paper introduces a Vessel Matrix Model (VMM) to CONA, which could present the natural properties of blood vessels.
- The model applies an RL algorithm to VMM to improve the targeting efficiency.

Future works may include accelerating the development of techniques to transform natural vessels into matrices and generate more datasets for training. It is also essential to generalize the current RL algorithm to train nanorobots and consider the dynamic conditions in the human environment.

References

1. Schulz, W.: Molecular Biology of Human Cancers: An Advanced Student's Textbook. Springer, Dordrecht, The Netherlands (2005)
2. Abubakar, I., Tillmann, T., Banerjee, A.: Global, regional, and national age-sex specific all-cause and cause-specific mortality for 240 causes of death, 1990–2013: A systematic analysis for the global burden of disease study 2013. Lancet **385**(9963), 117–171 (2015)
3. Bohunicky, B., Mousa, S.A.: Biosensors: the new wave in cancer diagnosis. Nanotechnol. Sci. Appl. **4**(1), 1–10 (2011)
4. Wilhelm, S., Tavares, A.J., Dai, Q., Ohta, S., Chan, W.C.W.: Analysis of nanoparticle delivery to tumours. Nat. Rev. Mater. **1**(5), 16014 (2016)
5. Kim, H., Cheang, U.K., Rogowski, L.W., Kim, M.J.: Motion planning of particle based microrobots for static obstacle avoidance. J. Micro-Bio Robot. (2018)
6. Okaie, Y., Nakano, T., Hara, T., Hosoda, K., Hiraoka, Y., Nishio, S.: "Modeling and performance evaluation of mobile bionanosensor networks for target tracking. In: Proceedings of IEEE International Conference Communication (ICC), Sydney, NSW, Australia, 2014, pp. 3969–3974 (2014)
7. Liu, L., Sun, Y., Shi, S., Chen, Y.: Smart tumour targeting by reinforcement learning. In: 2021 IEEE International Conference on Nano/Molecular Medicine and Engineering (NANOMED), Virtual, Nov. 15–18 (2021)
8. Ali, M., Chen, Y., Cree, M.J.: Autonomous in vivo computation in internet-of-nano-bio-things. IEEE Internet Things J. **9**(8), 6134–6147 (2021) https://doi.org/10.1109/JIOT.2021.3111089
9. Gazit, Y., et al.: Fractal characteristics of tumour vascular architecture during tumour growth and regression." Microcirculation (New York, N.Y. : 1994) **4**, 395–402 (1997). https://doi.org/10.3109/10739689709146803
10. Sun, Y., Zhang, R., Chen, Y.: A molecular communication detection method for the deformability of erythrocyte membrane in blood vessels. IEEE Trans. Nanobiosci. **20**(4), 387–395 (2021). https://doi.org/10.1109/TNB.2021.3064194
11. Wang, D., Sun, Y., Xiao, Y., Chen, Y.: An Optimal Strategy for Individualized Drug Delivery Therapy: A Molecular Communication Inspired Waveform Design Perspective, 2021 43rd Annual International Conference of the IEEE Engineering in Medicine & Biology Society (EMBC), pp. 866–869 (2021)https://doi.org/10.1109/EMBC46164.2021.9629560
12. McDougall, S.R., Anderson, A.R.A., Chaplain, M.A.J., Sherratt, J.A., et al.: Mathematical modelling of flow through vascular networks: Implications for tumour-induced angiogenesis and chemotherapy strategies[J]. Bull. Math. Biol. **64**, 673–702 (2022)

13. Wang, H., Yu, Y., Yuan, Q.: Application of dijkstra algorithm in robot path-planning. IEEE (2011)
14. Rahebi, J., HardalaÇ, F.: Retinal blood vessel segmentation with neural network by using gray-level co-occurrence matrix-based features. J. Med. Syst. **38**(8), 1–2 (2014)
15. Kaelbling, L.P., Littman, M.L., Cassandra, A.R.: Planning and acting in partially observable stochastic domains. Artif. Intell. **101**(1–2), 99–134 (1998)